Effect of driver to gate coupling circuits on EMI produced by SiC MOSFETS

J. Balcells , P. Bogónez-Franco
Electronics Department
Universitat Politècnica de Catalunya
08222 Terrassa, Spain
josep.balcells@upc.edu

***Abstract*—This work presents a study of the influence of different gate driver circuits on the switching behavior and EMI produced by SiC MOSFET devices used in a boost converter. The paper includes several simulations of switching behavior using different V_{GS} voltage levels and different passive RCD (Resistance Capacitor Diode) circuits to interface the driver to the SiC MOS gate and several tests of conducted and radiated EMI for each one of the interface circuits. The paper also includes a comparison of both aspects (switching and EMI) when using different gate voltage levels.**

The study reveals that gate voltage has little impact on switching behavior and therefore on conducted and radiated EMI, while gate RCD coupling circuits have a noticeable impact. The EMI reduction, when using the adequate driver-gate circuit may be in the order of 10 dB at certain frequencies in the conducted band and up to 20 dB for certain frequencies in the radiated band.

Keywords—SiC; EMI; conducted EM; radiated EMI; boost converter

I. INTRODUCTION

The benefits of SiC power semiconductors in comparison with Si in terms of blocking voltage [1], high temperature capability [2, 3], and lower on-resistance [4] has allowed their use in harsh environments like automotive, aerospace and wind-turbine generators [5, 6].

Despite those benefits some disadvantages exist, mainly those concerning the requirements of driver circuits to control the operation of SiC devices, especially in normally ON JFET devices.

In Si MOSFETs, to switch the device ON, the driver must supply a positive V_{GS} voltage higher than a certain threshold needed to saturate the device (V_{GSsat} , usually in the range of 15 to 20 V), while to turn it off, the driver must supply a V_{GS} voltage lower than a certain threshold voltage (V_{GSth}), greater than zero. Nevertheless, the V_{GS} voltage usually employed to block Si devices is 0 V. In case of SiC MOSFETs, the voltage needed to turn it ON is similar to the case of Si , but to turn it off, a negative voltage, between -2 V and -5 V, must be used [7]. This requires the use of special drivers and originates the need of driver supply sources having a negative output.

In this work we present a study describing the behavior of SiC devices when driven with different driver supply levels and with different circuits coupling the driver to gate. The paper presents several simulations with different driver to gate coupling circuits, in order to obtain the ON and OFF switching behavior and with the final aim of describing the EMI generated by SiC devices when driven with the different coupling circuits. The paper includes also a comparison between simulation and experimental results of ON and OFF switching processes, in order to validate the model of SiC MOSFET provided by the manufacturer. The test setup is based on a boost converter using a set of SiC transistor and diode.

II. TEST SETUP DESCRIPTION

Driver circuits, either for MOSFET or IGBT, have a great impact on the EMI behavior of power converters. To use as test setup for the study of the switching behavior if SiC devices, using different driver to gate coupling circuits, a boost converter was designed and has been simulated and tested. The semiconductors used in such boost converter (see schematic in Fig.1) have been the CMF20120D SiC MOSFET and the CD2F120F, SiC diode, both from CREE (USA).

The converter has an input voltage of 30 V_{DC} and an output voltage of 60 V_{DC}. The switching frequency used for the test was 100 kHz and the output power 120 W.

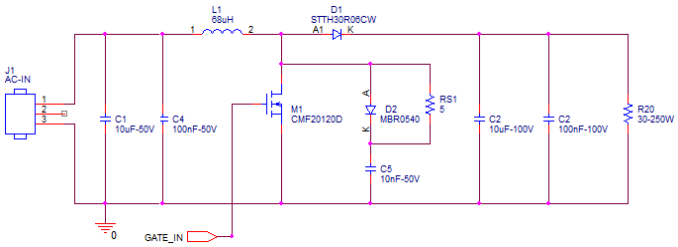

Fig. 1. Schematic of the boost converter.

This work has been performed with the financial support of Spanish Ministerio de Economia y Competitividad, in the frame of project CD2009-00046 belonging to Consolider-Ingenio Program.

Simulations using different V_{GS} voltages, where carried out, using OrCAD PSpice software. We obtained V_{DS} (drain to source voltage) and I_D (drain current) from simulations and also measured them, in order to validate the models, which were provided by the semiconductors manufacturer.

III. TEST VARIABLES AND CASES

Several tests changing key parameters (basically V_g and drive to gate coupling circuits) were performed. The test conditions are described in this paragraph and the results are described in the following paragraphs.

A. Driver to gate coupling resistor (R_g)

The coupling resistor between driver and gate has a great impact on switching characteristics of the MOSFET. As R_g increases, it limits the peak of current provided by the driver, and causes an increase of MOSFET turn-on and turn-off times. Nevertheless, as it will be seen, this helps reducing ringing in V_{GS} voltage. Four test cases were explored, with R_g values of 0 Ω, 5 Ω , 10 Ω and 15 Ω. In all the cases V_g swing was from -2 V to 20 V. Fig. 2 shows the driver to gate coupling circuit.

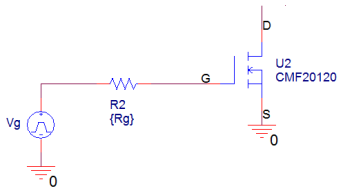

Fig. 2. Driver to gate coupling resistor.

B. V_g (gate supply voltage)

The SiC MOSFET manufacturer recommends in the datasheets [7] a V_{GS} voltage of +20 V to turn it on and -2 to -5 V to turn it off. Two simulations using V_g negative bias of -2 V and -5 V were carried out. In both cases the driver to gate coupling resistor was 0 Ω.

C. Parallel RC coupling circuit

Another set of tests were performed using a parallel RC coupling circuit. This configuration helps to improve the turn-off time. The capacitor charges at positive gate voltage and at turn-off this voltage adds to the negative voltage applied. Fig. 3 shows the RC coupling circuit. The gate resistor, R_g, was fixed to 5 Ω, and four cases were simulated changing the C_g to the following values: 100 pF, 1 nF, 10 nF and 100 nF.

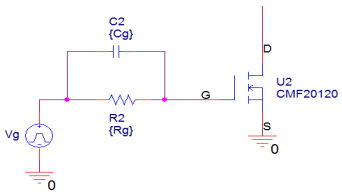

Fig. 3. Parallel RC coupling circuit.

D. Parallel RD coupling circuits for turn-on and turn-off

In order to control the turn-on and turn-off switching independently, a different gate resistor could be used. This can be achieved using a driver to gate coupling circuit combining two resistor-diode circuits (RD) and a simple resistor in parallel, Fig. 4 shows the RD coupling circuit. Resistor R_{ton} and diode D1 are active at turn-on and resistor and R_{toff} and diode D2 are active at turn-off. Four test cases were explored with R_g = 20 Ω, R_{ton} = 0 Ω and R_{toff} = 0, 5, 10 and 15 Ω . Fig. 4 shows the driver to gate coupling circuit.

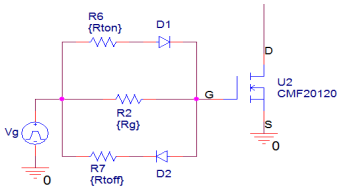

Fig. 4. Parallel RD (Resistance Diode) coupling circuit

IV. TEST RESULTS

This paragraph presents the experimental results obtained with the different setups described in the previous paragraph. Three kinds of parameters were the focus of interest:

a) ON and OFF switching behavior, presented by means of time domain signals of V_{DS} and I_D.

b) Conducted EMI, measured by means of a LISN.

c) Radiated EMI, measured by means of a GTEM cell (Wavecell from Wavecontrol, Spain).

The EMI receiver used for conducted and radiated measurements was an ESPI-3 from Rohde&Schwarz.

A. Influence of gate resistor

Gate resistor effect in switching characteristics is shown in Fig. 5. The resistor values simulated, R_g, were 0 Ω (blue trace), 5 Ω (red trace), 10 Ω (pink trace), 15 Ω (black trace) and 20 Ω (green trace) (V_g swing from -2 V to 20 V). We can see that as gate resistor increases, the turn-on and turn-off times increase and drain current ringing decreases. There is a maximum value for such resistor, since values higher than 10 Ω cause a great distortion in gate voltage and high power losses.

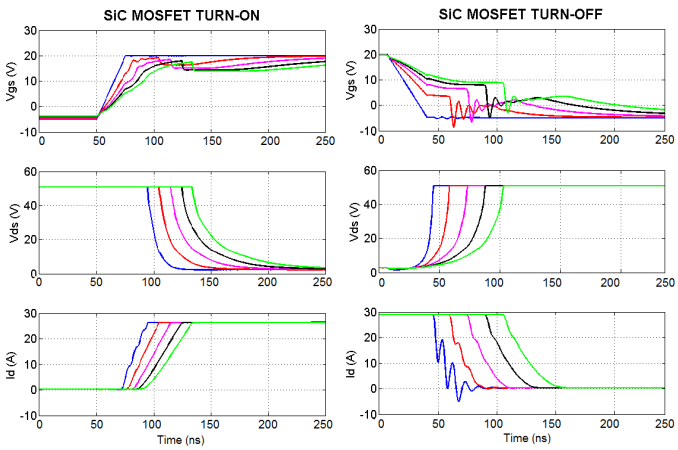

Fig. 5. Effect of the series gate resistor on switching characteristics (simulation results). Cases: R_g = 0 Ω (blue trace), R_g = 5 Ω (red trace), R_g = 10 Ω (pink trace), R_g = 15 Ω (black trace) and R_g = 20 Ω (green trace).

In order to validate the model supplied by the manufacturer, we made a real test on the prototype, measuring V_{GS} and V_{DS} with an oscilloscope. The results are presented in Fig.6 where we can observe great differences between simulation and measurements in the detail of transient behavior, mainly of V_{GS}. Nevertheless, rise and fall times of V_{DS} approach reasonably well. That means that the model provided by the manufacturer is not valid to predict the HF noise due to ringing. Since ringing is in the order of 10 ns, that means that EMI predictions will probably fail above 100 MHz, which is out of the band of interest for conducted EMI.

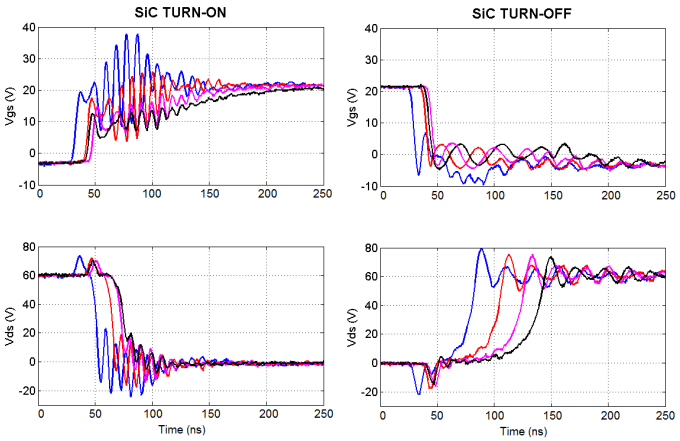

Fig. 6. Effect of the series gate resistor on switching characteristics (experimental results). Cases: R_g = 0 Ω (blue trace), R_g = 5 Ω (red trace), R_g = 10 Ω (pink trace) and R_g = 15 Ω (black trace).

Fig. 7 shows the conducted EMI measured for the different cases described above. We can see that using a 15 Ω resistor, we obtain a maximum reduction of 10 dB at 6 MHz and lower reductions in the range from 4 MHz to 15 MHz. In the rest of the spectrum of conducted EMI there are no significant differences for different driver to gate resistor values.

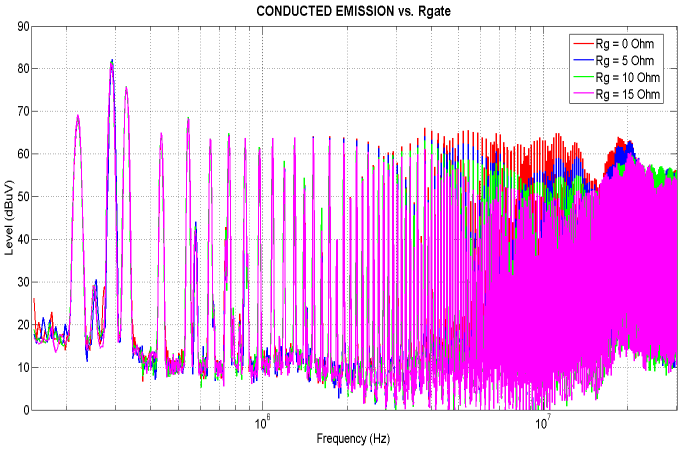

Fig. 7. Effect of the series resistor on conducted EMI (experimental results). Cases: R_g = 0 Ω (red trace), R_g = 5 Ω (blue trace), R_g = 10 Ω (green trace) and R_g = 15 Ω (pink trace) were used.

Fig. 8 shows radiated EMI for the same cases explored above with different gate resistors. A reduction of EMI in the range from 90 MHz to 350 MHz is observed for high values of gate resistor (15 Ω). The average reduction is 10 dB and a maximum reduction of 20 dB can be observed at 220 MHz.

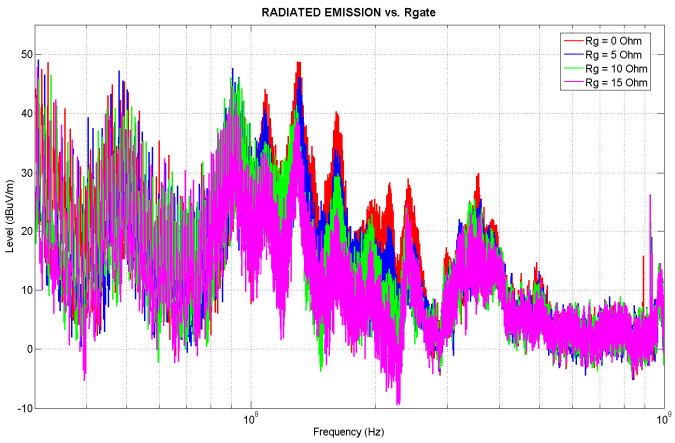

Fig. 8. Effect of the series resistor on radiated EMI (experimental results). Cases: R_g= 0 Ω (red trace), R_g=5 Ω (blue trace), R_g=10 Ω (green trace) and R_g=15 Ω (pink trace).

B. *Influence of the gate voltage*

Negative bias of the gate has a great effect on switching characteristics. Fig. 9. Shows the time domain response obtained by simulation with different values. The explored cases were: *Vg* = 0 to 20 V (blue trace), *Vg* = -2 to 20 V (red trace) and *Vg* = -5 to 20 V (green trace). With zero negative bias we can observe some ringing in the current turn-off. The ringing disappears as negative bias increases, but this penalizes the turn on delay.

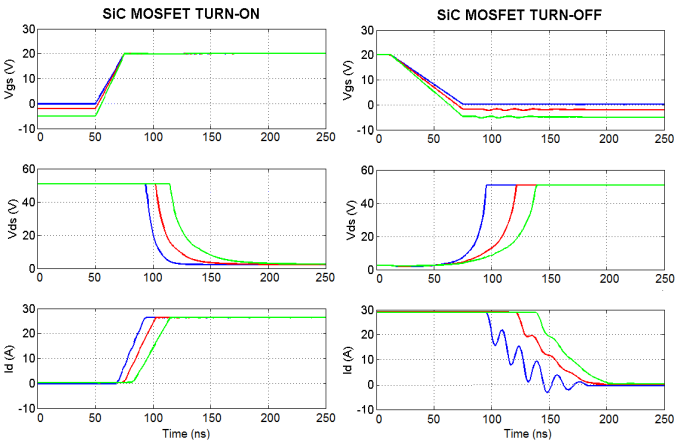

Fig. 9. Effect of the gate voltage on switching characteristics (simulation results). Cases: V_g = 0 V to 20 V (blue trace), V_g = -2 V to 20 V (red trace) and V_g = -5 V to 20 V (green trace).

Fig. 10 shows the conducted EMI for the different cases of gate bias voltage. A negative bias of -5 V causes a reduction of 8 dB in the range from 7 MHz to 10 MHz. This reduction is not significant (in the order of magnitude of error). In the rest of

the spectrum, the conducted EMI have the same value, independently of the gate voltage.

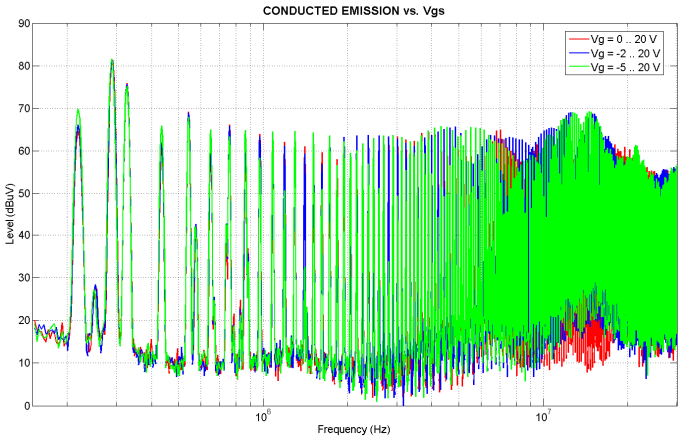

Fig. 10. Effect of the gate voltage on conducted EMI (experimental results). Cases: V_g = 0 to 20 V (blue trace), V_g = -2 to 20 V (red trace) and V_g = -5 to 20V (green trace).

Fig. 11 shows the effect of the different gate voltages described previously on radiated EMI. From this graph we can see that gate voltage has no effect on the radiated EMI.

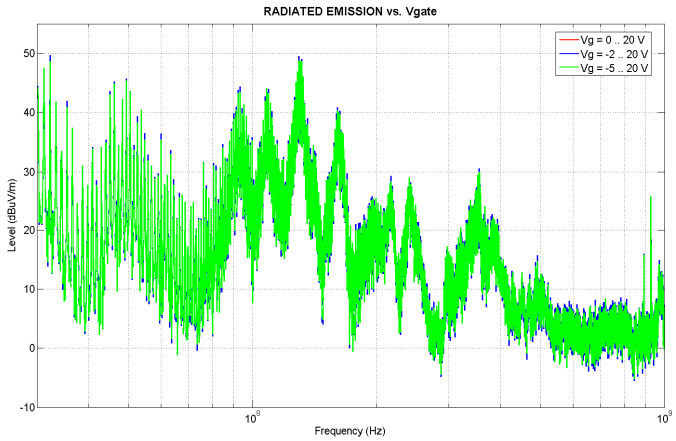

Fig. 11. Effect of the gate voltage on radiated EMI (experimental results). Cases: V_g =0 to 20 V (blue trace), V_g = -2 to 20 V (red trace) and V_g = -5 to 20 V (green trace).

C. *Parallel RC coupling circuit*

Fig. 12 shows the switching behavior with RC coupling circuit shown in Fig. 3. Gate resistor was fixed to 5 Ω for all simulations and the capacitor values tested were 100 pF, 1 nF, 10 nF, 100 nF. Gate voltage was fixed to -2 V to 20 V. As capacitor value increases, turn-on and turn-off times increase and ringing in drain current is reduced, but no eliminated. For the higher capacitor values, 10 nF and 100 nF, turn-off V_{GS} is highly distorted.

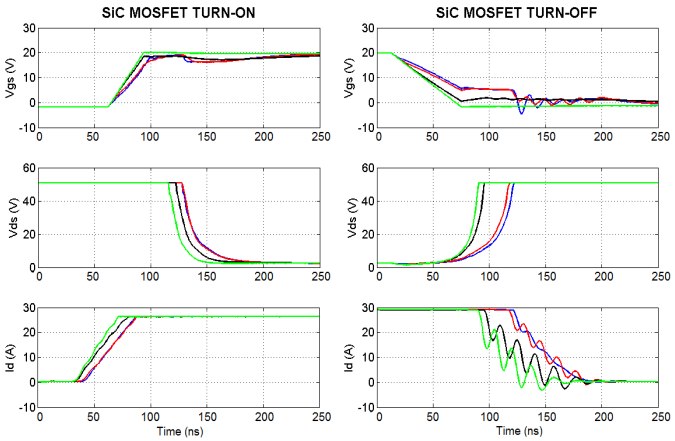

Fig. 12. Effect of RC coupling circuit on switching characteristics (simulated results). Cases: Cg = 100 pF (green trace), Cg = 1 nF (black trace), Cg = 10 nF (red trace), Cg = 100 nF (blue trace).

Fig. 13 shows the conducted EMI for the different cases of RC circuits described above. There is a reduction in conducted EMI in the range of 5 to 20 MHz. A maximum reduction of 10 dB is achieved in the frequency range from 7 MHz to 15 MHz with C_g= 100 nF. For the rest of the spectrum the conducted EMI remains the same.

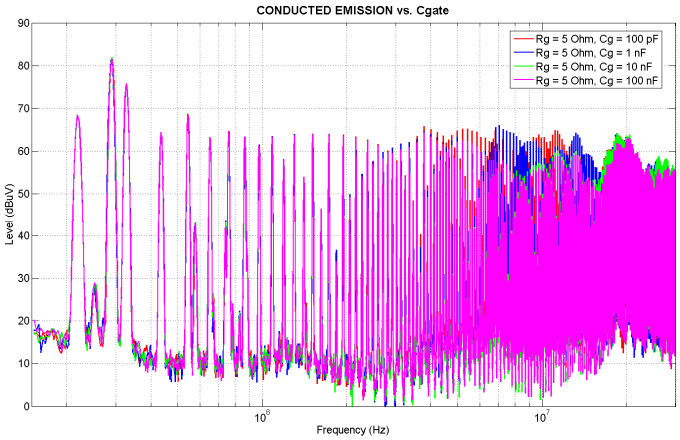

Fig. 13. Effect of RC coupling circuit on conducted EMI (experimental results). Cases: Cg = 100pF (red trace), Cg = 1 nF (blue trace), Cg = 10 nF (green trace), Cg = 100 nF (pink trace).

Fig. 14 shows the radiated EMI for different RC coupling circuits. Reduction in radiated EMI occurs between 180 MHz and 250 MHz. The bigger reduction, 18 dB, occurs at 220 MHz with Cg =100 nF. The reduction is similar to that achieved with high values of R_g, and both are due to the slower response during the switching.

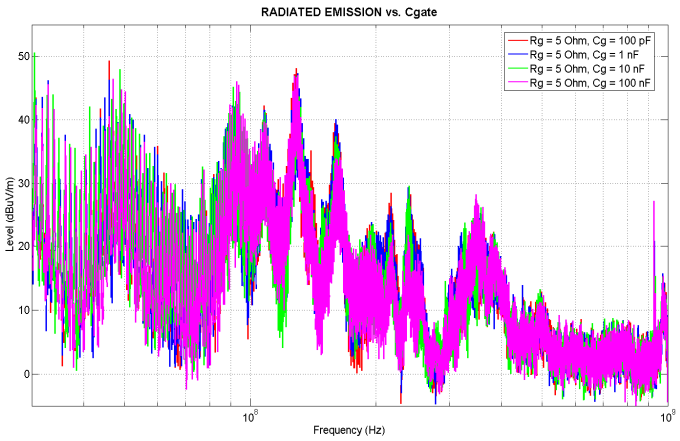

Fig. 14. Effect of RC coupling circuit on radiated emissions (experimental results). Cases: Cg = 100pF (red trace), Cg = 1 nF (blue trace), Cg = 10 nF (green trace), Cg = 100 nF (pink trace).

D. Parallel RD coupling circuits for turn-on and turn-off

Fig. 15 shows the switching characteristics when using the coupling circuit of fig 4. In this simulation the turn-on resistor, R_{ton}, was fixed to 0 Ω, the gate resistor, R_g, to 20 Ω and we experimented with different values of turn-off resistor, R_{toff}. The tested values were 0 Ω, 5 Ω, 10 Ω and 15 Ω. Gate voltage swing was V_g=-2 V to 20 V. As expected, the turn-on time is the same for all the simulations and the effect is clearly visible at the turn-off time. As R_{toff} is increased, V_{GS} is more and more distorted, the turn-off times increase and the drain current ringing diminishes.

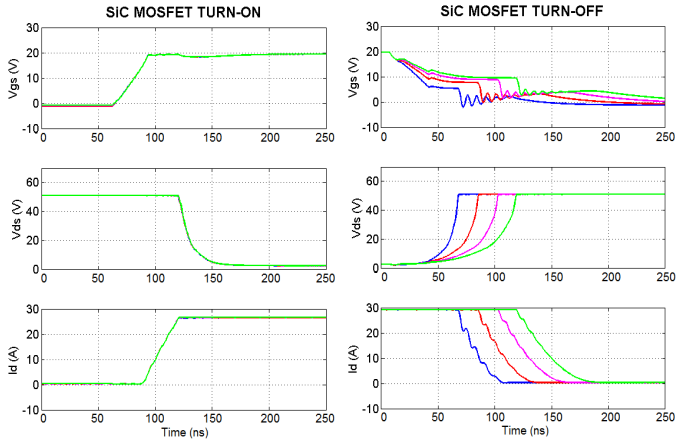

Fig. 15. Effect of parallel RD coupling circuit on switching characteristics (simulated results). Cases: R_{toff} = 0 Ω (blue trace), R_{toff} = 5 Ω (red trace R_{toff} = 10 Ω (pink trace) and R_{toff} = 15 Ω (green trace).

Fig. 16 shows the conducted EMI for different R_{toff} values. There are no significant differences with the different RD coupling circuits. The maximum reduction observed is about 6 dB, which is in the order of magnitude of error.

Fig. 17 shows radiated EMI for different RD coupling circuits. A slight reduction occurs between 200 MHz and 600 MHz. Maximum reduction observed is 12 dB when R_{toff} is 15Ω. The use of resistors greater than 5 Ω have a similar effect.

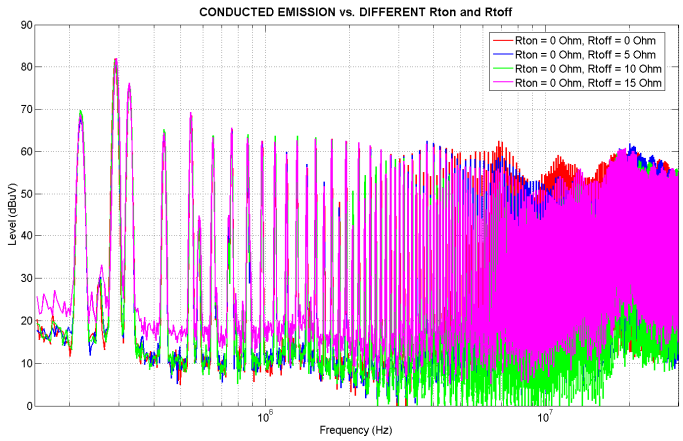

Fig. 16. Effect of parallel RD coupling circuit on conducted EMI (experimental results). Cases: R_{toff} = 0 Ω (blue trace), R_{toff} = 5 Ω (red trace), R_{toff} =10 Ω (pink trace) and R_{toff} = 15 Ω (green trace).

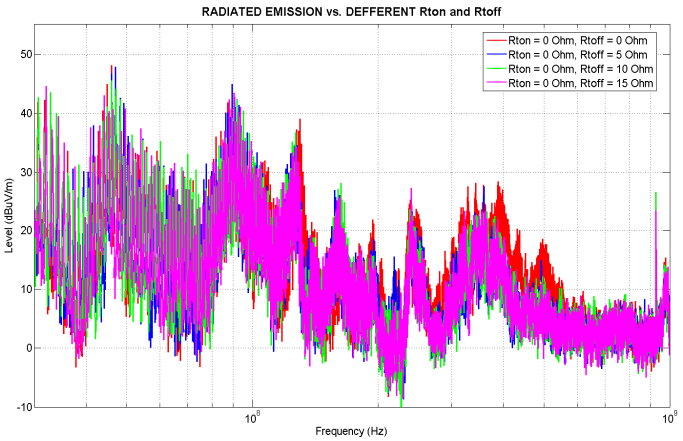

Fig. 17. Effect of parallel RD coupling circuit on radiated EMI (experimental results). Cases: R_{toff} = 0 Ω (blue trace), R_{toff} = 5 Ω (red trace), R_{toff} =10 Ω (pink trace) and R_{toff} = 15 Ω (green trace).

V. CONCLUSIONS

Negative bias of SiC devices has minimal impact on conducted and radiated EMI generated by the converters, even though it has some impact on the switching times.

The use of driver to gate coupling circuits allows small improvements in the EMI behavior.

Using a simple gate resistor as coupling circuit produces the major impact on the conducted and radiated EMI. Reduction in the order of 10 dB in conducted EMI and 20 dB in radiated EMI can be expected with gate resistors in the order of 15 Ω.

Using parallel RC or RCD coupling circuits does not improve significantly the behavior of a simple resistor.

As a collateral conclusion we also observed that SPICE model provided by the manufacturer doesn't give good results to obtain the MOSFET switching behavior, especially predicting the effects of gate capacitances and Miller effect.

ACKNOWLEGEMENT

This work has got the financial support of Spanish Ministerio de Economia y Competitividad, in the frame of project CD2009-00046 belonging to Consolider-Ingenio Program and also project TEC2011-25076.

REFERENCES

[1] V. Veliadis, M. Snook, T. McNutt, H. Heame, P. Potyraj, A. Lelis and C. Scozzie, “A 2055-V (at 0.7 mA/cm2) 24-A (at 706 W/cm) Normally On 4H-SiC JFET With 6.8-mm2 Active Area and Blocking-Voltage Capability Reaching the Material Limit *Electron Device Letters, IEEE*, vol.29, no.12, pp.1325-1327, Dec. 2008

[2] T. Funaki, J.C. Balda, J. Junghans, A.S. Kashyap, H.A. Mantooth, F. Barlow, T. Kimoto and T. Hikihara, "Power Conversion With SiC Devices at Extremely High Ambient Temperatures," *Power Electronics, IEEE Transactions on* , vol.22, no.4, pp.1321-1329, July 2007

[3] R. Wang, P. Ning, D. Boroyevich, M. Danilovic, E. Wang, R. Kaushik, “Design of high-temperature SiC three-phase AC-DC converter for >100ºC ambient temperature,” *Proc. Energy Conversion Congress and Exposition ECCE*, Atlanta, USA, 2010, pp. 1283-1289.

[4] P. Friedrichs, H. Mitlehner, K.O. Dohnke, D. Peters, R. Schorner, U. Weinert, E. Baudelot and D. Stephani, "SiC power devices with low on-resistance for fast switching applications," *Power Semiconductor Devices and ICs, 2000. Proceedings. The 12th International Symposium on*, pp.213-216, 2000

[5] D. Bortis, B. Wrzecionko and J.W. Kolar, "A 120°C ambient temperature forced air-cooled normally-off SiC JFET automotive inverter system," *Applied Power Electronics Conference and Exposition (APEC), 2011 Twenty-Sixth Annual IEEE*, pp.1282-1289,March 2011.

[6] Z. Hui and L.M. Tolbert, "Efficiency Impact of Silicon Carbide Power Electronics for Modern Wind Turbine Full Scale Frequency Converter," *Industrial Electronics, IEEE Transactions on*, vol.58, no.1, pp.21-28, Jan. 2011

[7] CMF20120D - Silicon Carbide power MOSFET datasheet. CREE Ind. Rev. D. 2012.